UNIVERSITAT POLITÈCNICA DE CATALUNYA
BARCELONATECH
Facultat d'Òptica i Optometria de Terrassa

MÀSTER UNIVERSITARI EN OPTOMETRIA I CIÈNCIES DE LA VISIÓ

TREBALL FINAL DE MÀSTER

HYPERSPECTRAL RETINOGRAPHY: EFFECTS OF AGING IN HEALTHY ADULTS

NÚRIA MARTINEZ BARNIOL

MERITXELL VILASECA RICART
FRANCISCO BURGOS FERNANDEZ
DEPARTAMENT D'ÒPTICA I OPTOMETRIA

14 de febrer de 2020

Facultat d'Òptica i Optometria de Terrassa

Declaració de confidencialitat dels treballs acadèmics (TFG, TFM, etc.)

IDIOMA DEL TFC *ANGLÈS*

Declaració de confidencialitat

En/Na Meritxell Vilaseca, com a professor/a responsable de la direcció, coordinació i/o tutoria del treball acadèmic dipositat per l'estudiant Núria Martínez Barniol titulat "Hyperspectral retinography: effects of aging in healthy adults" declaro que:

(X) el treball acadèmic **és confidencial** (segons les condicions detallades a continuació)

( ) el treball acadèmic **no és confidencial**

Període i motius de la confidencialitat

[Ompliu aquest apartat només si heu declarat que el treball és confidencial]

El sotasignant declara que el treball acadèmic ha de ser confidencial pel període de temps indicat a continuació:

(X) **fins a la data** 14 de febrer de 2024

( ) la durada de la confidencialitat és **indefinida**

El sotasignant declara que els motius d'aquesta confidencialitat són:

( ) es vol avaluar la possibilitat de protegir el treball

( ) un tercer manifesta interès en comercialitzar el treball

( ) forma part d'un treball de recerca amb una empresa que està subjecte a confidencialitat

(X) altres El treball forma part d'un projecte de recerca del qual es volen publicar part dels resultats

Difusió pública del treball confidencial

[Ompliu aquest apartat només si heu declarat que el treball és confidencial]

El sotasignant autoritza la difusió del treball confidencial al dipòsit institucional a *UPCommons* o plataforma que el substitueixi sota aquestes condicions:

(X) difusió del **text complet del treball** a partir de la data d'embargament indicada a l'apartat anterior (sempre i quan l'autor del treball autoritzi aquesta difusió)

( ) difusió única de les **dades bibliogràfiques** del treball (sense el text complet)

( ) la confidencialitat del treball no permet **cap difusió** del mateix

En cas que la confidencialitat del treball no permeti cap difusió del mateix, el Servei de Biblioteques, Publicacions i Arxius de la UPC, acollint-se a l'article 37.1 de la *Llei de Propietat Intel·lectual*, dipositarà en tancat el projecte a *UPCommons* (sense cap accés públic al text ni corresponents dades bibliogràfiques), garantint-ne així la seva confidencialitat, preservació i conservació.

Terrassa, 23 de gener de 2020

Signatura del professor director, coordinador i/o tutor:

UNIVERSITAT POLITÈCNICA DE CATALUNYA
BARCELONATECH
Facultat d'Òptica i Optometria de Terrassa

MÀSTER UNIVERSITARI EN OPTOMETRIA I CIÈNCIES DE LA VISIÓ

Els Drs. Meritxell Vilaseca i Francisco J. Burgos, com a directors del treball

CERTIFIQUEN

Que la Sra. Núria Martínez Barniol ha realitzat sota la seva supervisió el treball **"Hyperspectral retinography: effects of aging in healthy adults"** que es recull en aquesta memòria per optar al títol de màster en optometria i ciències de la visió.

I per a què consti, signem aquest certificat.

Dra. MERITXELL VILASECA
Directora del treball

Dr. FRANCISCO J. BURGOS
Co-director del treball

Terrassa, 20 de gener de 2020

UNIVERSITAT POLITÈCNICA DE CATALUNYA
BARCELONATECH
Facultat d'Òptica i Optometria de Terrassa

MÀSTER UNIVERSITARI EN OPTOMETRIA I CIÈNCIES DE LA VISIÓ

RETINOGRAFIA HIPERESPECTRAL: EFECTES DE L'EDAT EN PACIENTS ADULTS SANS

RESUM

Propòsit: Validar una càmera de fons d'ull hiperespectral amb sensibilitat en el rang de llum visible i infraroig proper, com un mitjà per obtenir informació espectral del fons d'ull i els efectes de l'envelliment en pacients adults sans.

Mètodes: Un total de 105 ulls sans, de pacients d'entre 30 i 89 anys d'edat, van ser inclosos a l'estudi. A tots ells se'ls va realitzar un examen optomètric. A més, es van fer mesures amb retinograf de color convencional, amb tomografia de coherència òptica i amb càmera de fons d'ull hiperespectral.

Resultats: Els resultats van mostrar valors de reflectància més alts a longituds d'ona curtes en pacients d'edats avançades (entre 70 i 89 anys) respecte la resta. Dins d'aquest rang d'edat, els pacients avaluats tenien implantada una per cirurgia de cataractes i, per aquesta raó, tenien major transparència dels medis oculars. En els altres grups d'edat, la reflectància tendia a disminuir amb l'edat. D'altra banda, depenent de les longituds d'ona analitzades, les imatges van ressaltar diferents estructures oculars. Les longituds d'ona més curtes, de 416nm a 525nm, van revelar informació sobre les fibres nervioses i el disc òptic. Les longituds d'ona entre 595nm i 732nm van ser útils per ressaltar estructures vasculars. Finalment, les longituds d'ona més llargues (>865nm) van mostrar informació sobre estructures més profundes, com els vasos coroidals.

Conclusions: S'ha demostrat que les imatges hiperespectrals són útils per proporcionar informació de diferents estructures oculars. Les corbes de reflectància han permès avaluar de manera quantitativa la possible reducció de la transparència dels medis oculars, així com informació rellevant de les estructures del fons d'ull. Així, aquest instrument podria ser útil clínicament per al diagnòstic precoç i el seguiment de malalties oculars que afecten la retina.

UNIVERSITAT POLITÈCNICA DE CATALUNYA
BARCELONATECH
Facultat d'Òptica i Optometria de Terrassa

MÀSTER UNIVERSITARI EN OPTOMETRIA I CIÈNCIES DE LA VISIÓ

RETINOGRAFIA HIPERESPECTRAL: EFECTOS DE LA EDAD EN PACIENTES ADULTOS SANOS

RESUMEN

Propósito: Validar una cámara de fondo de ojo hiperespectral con sensibilidad en el rango de luz visible e infrarrojo cercano, como un medio para obtener información espectral del fondo de ojo y los efectos del envejecimiento en pacientes adultos sanos.
Métodos: Un total de 105 ojos sanos, distribuidos en diferentes rangos de edad (30-89 años), se incluyeron en un estudio clínico. A todos los pacientes se les realizó un examen optométrico. Además, se llevaron a cabo medidas con retinógrafo de color convencional, con tomografía de coherencia óptica y con la cámara de fondo hiperespectral.
Resultados: Los resultados mostraron valores de reflectancia más altos a longitudes de onda cortas en pacientes de edad avanzada (entre 70 y 89 años) con respecto al resto. Dentro de este rango de edad, todos los pacientes tenían implantada una lente por cirugía de cataratas y, por esta razón, tenían una mayor transparencia de los medios oculares. En los otros grupos de edad, la reflectancia tendía a disminuir con la edad. Por otro lado, dependiendo de las longitudes de onda analizadas, las imágenes resaltaron diferentes estructuras oculares. Las longitudes de onda más cortas, de 416 nm a 525 nm, revelaron información sobre las fibras nerviosas y el disco óptico. Las longitudes de onda entre 595 nm y 732 nm fueron útiles para resaltar estructuras vasculares. Finalmente, las longitudes de onda más largas (>865 nm) mostraron información sobre estructuras más profundas, como los vasos coroideos.
Conclusiones: Se ha demostrado que las imágenes hiperespectrales son útiles para proporcionar información sobre diferentes estructuras oculares. Las curvas de reflectancia han permitido evaluar de manera cuantitativa la posible reducción de la transparencia de los medios oculares, así como información relevante de las estructuras del fondo de ojo. Así, estos dos factores respaldan el hecho de que este instrumento podría ser útil clínicamente para el diagnóstico precoz y el seguimiento de enfermedades oculares que afectan la retina.

UNIVERSITAT POLITÈCNICA DE CATALUNYA
BARCELONATECH
Facultat d'Òptica i Optometria de Terrassa

MÀSTER UNIVERSITARI EN OPTOMETRIA I CIÈNCIES DE LA VISIÓ

HYPERSPECTRAL RETINOGRAPHY: EFFECTS OF AGING IN HEALTHY ADULTS

SUMMARY

Purpose: To validate a hyperspectral fundus camera, which has sensitivity in the visible and the near-infrared ranges, as a means of obtaining spectral information of the fundus and the effects of aging in healthy adult patients.

Methods: A total of 105 healthy eyes, distributed in different ranges of age (30-89 years old), were included in a clinical study. All patients were examined with the usual optometric exam. Additionally, measurements with conventional colour retinography, optical coherence tomography and hyperspectral fundus camera were carried out.

Results: The results showed that the spectral reflectance at shorter wavelengths of patients between 70 and 89 years was higher with respect to the others. Within this age range, all the patients had been previously implanted with intraocular lenses and, for this reason, they had higher ocular media transparency. On the other hand, depending on the wavelengths analysed, the images highlighted different ocular structures. The shorter wavelengths, from 416nm to 525nm, revealed information about nervous fibres and also the optic disc. Wavelengths between 595nm and 732nm were useful to highlight vascular structures. Finally, the longer wavelengths (>865nm) showed information about deeper structures, like the choroidal vasculature.

Conclusions: Hyperspectral images were shown to be useful to provide information about different ocular structures. The reflectance curves allowed us to evaluate in a quantitative way the possible reduction of ocular media transparency as well as other relevant information from ocular structures. These two factors support the fact that this instrument might be clinically useful to early diagnose and follow up several eye diseases affecting the retina.

Hyperspectral Retinography: effects of aging in healthy adults

NÚRIA MARTINEZ BARNIOL

Center for Sensors, Instruments and Systems Development, Technical University of Catalonia, Rambla de Sant Nebridi 10, Terrassa, 08222, Spain

* nuriamartinezbarniol@gmail.com

Abstract: A hyperspectral fundus camera, which has sensitivity in the visible but also in the near-infrared range (400nm – 1300nm), has been used in this study as a means of obtaining spectral information of the fundus and the effects of aging in healthy adult patients. A total of 105 healthy eyes from 60 patients, distributed in different ranges of age (30-89 years old), were included in the clinical study. The results showed that the shorter wavelengths (416nm-525nm) revealed information about nervous fibers and optic disc. Wavelengths between 595nm-732nm were useful to highlight vascular structures, like arteries and veins. Finally, the longer wavelengths (>865nm) showed information about deeper structures, like the choroid vasculature. Also, results mainly showed differences in terms of spectral reflectance in patients between 70 and 89 years with respect to those of other decades of age. All the oldest patients evaluated had been previously implanted with intraocular lenses and, for this reason, they had unexpected higher ocular media transparency. In the other age groups, the reflectance generally decreased as the age increased. These results support the fact that this instrument might be useful clinically to early diagnose and follow up several eye diseases affecting the retina.

1. Introduction

According to demographic development, life expectancy is increasing notably, which means that individuals might suffer a deterioration of the visual health more commonly and have higher risk of ocular pathology. There are many eye diseases that appear with age: patients above the age of 70 years have higher risk of developing diseases like cataracts, Age-related Macular Degeneration (AMD), glaucoma, diabetic retinopathy and retinal detachment (RD) than those between the ages of 50 and 70 [1]. Considering all this, control revisions and early diagnosis become very important, especially in old-aged individuals.

In particular, retinal and Optic Nerve Head (ONH) diseases can cause vision loss and blindness [2] if they are not diagnosed in time. Due to the prevalence of these ocular pathologies, it is therefore of particular interest and relevance to use a retinal observation method allowing their detection and early diagnosis in clinics. Nowadays, a set of tests and exams are performed at the optometric or ophthalmic visits with the aim of evaluating the eye health as a whole, establishing a treatment if needed. One of the most important tests is the observation of the posterior pole, which can be done by means of different optical imaging systems. The most common ones are those based on fundus photography [3], fluorescein angiography [4], infrared imaging [5], and Optical Coherence Tomography (OCT) [6]. All of them are non-invasive techniques and may enhance detection of retinal lesions compared with only the traditional fundus examination through an ophthalmoscope [7].

During the progression of degenerative retinal pathologies, like AMD, diabetic retinopathy or glaucoma, different stages can be distinguished, where at the most initial phases none or few pathological signs can be observed using the most common imaging systems. The conventional fundus cameras are based on RGB imaging systems with only three spectral bands: red, green and blue. These systems include one trichromatic camera with a white light source [8]. More recently, HYperspectral imaging Systems (HYS) have been introduced allowing the acquisition of spectral images through more than 3 spectral bands, modifying the spectral sampling in comparison with common fundus camera by means of changes in the illumination or acquisition bands. There are systems in which tuneable filters have been placed in front of a monochromatic camera [9,10], or alternatively others use Light Emitting Diodes (LED) [11,12] or sequential HYS sensors based on band-pass interference filters [13]. These instruments, even though they show some improvement with respect to conventional RGB cameras, only allow the acquisition of images within the visible range. Additionally, they are susceptible of generating severe motion artefacts and pixel misregistration because the eye is constantly moving and the acquisition time is rather long.

For this reason, a HYS fundus camera that has been recently developed at the Universitat Politècnica de Catalunya (UPC) - Centre for Sensors, Instruments and Systems Development (CD6) has been used in this study, which has sensitivity in the visible but also in the near-infrared range (400nm – 1300nm). This system is useful to acquire images with more detailed information of retinal deeper layers, even reaching the choroid (choroidal vasculature and the Retinal Pigment Epithelium, RPE). This part of the retina cannot be observed with trichromatic fundus cameras because visible light does not penetrate so deep due to high absorbance of the preceding layers. The system is able to perform fast imaging of the retina and is expected to provide relevant spectral information of deeper structures of the retina from the images taken within 900nm and 1300nm, as in this range there is less absorption of melanin and hemoglobin [14].

The goal of this study is to clinically validate the new HYS fundus camera prototype in healthy patients aged from 30 years to 89 years, as a means of evaluating the spectral features of different retinal structures over time and possibly detect some pathological signs that sometimes are ignored using conventional retinography. The study underlines the clinical potential of this system as a new tool for ophthalmic diagnosis [15].

2. Material and methods

2.1. HYS fundus camera

The HYS fundus camera used for this study is composed by lenses, mirrors, diaphragms, LEDs and two cameras (Fig. 1). The first is a CMOS camera (Orca Flash 4.0, Hamamatsu, Japan) with 2048x2048 pixels, with sensitivity to visible (VIS) light (400nm - 1000nm). The second is a camera called InGaAs (C12741-03, Hamamatsu, Japan) with 640x512 pixels, with sensitivity to near infrared (NIR) light (950nm - 1700nm). Both cameras are synchronized and for this reason, all spectral images are obtained in 613ms (154ms for the CMOS and 459ms for the InGaAs). As it is a fast capture, it prevents from invalid images due to the patient's ocular movements. The whole prototype has an angular field of view of 30º of the fundus and magnifications of 1.20 (VIS) and 0.88 (NIR), which allow taking images of the eye fundus without the prior need to dilate the patient's pupil with mydriatic drops.

The main feature of this fundus camera is that it is made up of light sources composed of LEDs emitting at different regions of the VIS and NIR spectrum allowing 15 different images to be obtained at 15 spectral bands centred at the following wavelengths: 416nm, 450nm, 471nm, 494nm, 525nm, 595nm, 598nm, 624nm, 660nm, 732nm, 865nm, 955nm, 1025nm, 1096nm and 1213nm. The shorter wavelengths enable to analyse in detail the most superficial retinal structures, such as nerve fibres, while the infrared ones allow the visualization of deeper layers of the back of the eye, such as the choroid.

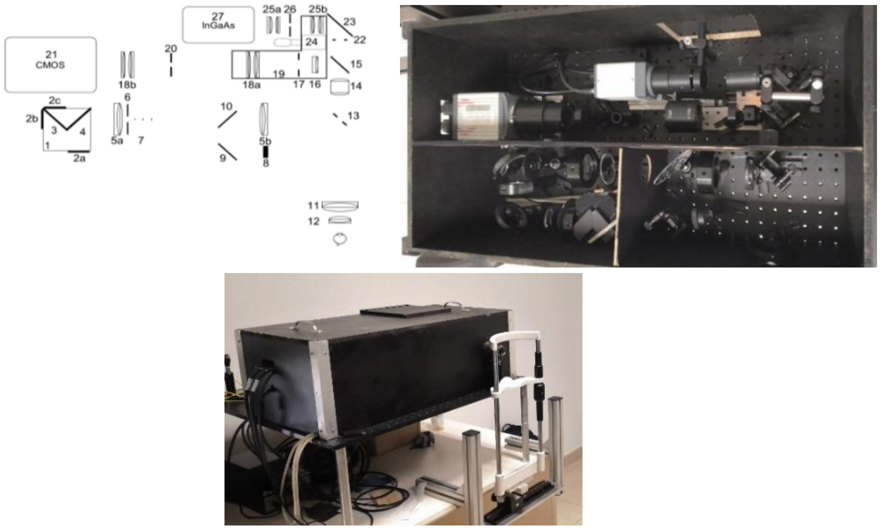

Fig. 1. Optical scheme of the HYS fundus camera (Top left). Illumination arm: 1-LED rings structure; 2a, 2b, 2c-LED rings; 3, 4-1150 nm and 700 nm dichroic mirrors; 5a, 5b-Illumination telescopes' lenses; 6-Retinal conjugated diaphragm; 7-Anti-backreflections stops; 8-Fixation target; 9-Mirror; 10-Beam splitter plate. Detection arms: 11, 12-Objective's lenses; 13-Holed mirror; 14-Lens; 15-950 nm dichroic mirror. VIS-NIR detection path: 16-Lens; 17-Field diaphragm; 18a, 18b-VIS-NIR telescope's lenses; 19-Refraction correction translator platform; 20-Aperture diaphragm; 21-CMOS camera. NIR detection path: 22-Field diaphragm; 23-Mirror; 24-Platform-linear translator; 25a, 25b-NIR telescope's lenses; 26-Aperture diaphragm; 27-InGaAs camera. Internal view of the HYS fundus camera (Top right). External view of the HYS fundus camera (Bottom).

2.2. Control software

To acquire the spectral images, two programs were simultaneously used together with the HYS fundus camera: the HoKaWo and MATLAB R2018b (Fig. 2). The first one allowed us to control both cameras, to obtain an optimal visualization of the posterior pole, and to adjust some parameters needed for the acquisition, the so-called Look Up Table (LUT), in order to highlight the ocular fundus structures while minimizing the back reflections of the system. It is to be highlighted that back reflections are one of the main drawbacks in fundus cameras as the retina reflects only about 3% of the energy while back reflections of optical surfaces included in the components of the camera as well as in the eye itself (such as the cornea and the lens) might be much stronger. Therefore, they must be avoided if usable spectral information is to be obtained from the retinal and choroidal structures. The second program allowed us to select the right and left eye, save the patient's refraction (spherical equivalent), and perform the corresponding adjustment on a micrometric screw of the system to compensate for the refractive state of every patient. The program actually indicates the number of millimetres (mm) that permit to correct the patient's spherical refraction to obtain focused fundus images. Finally, once the images have been taken, they are displayed using the Fiji program (ImageJ).

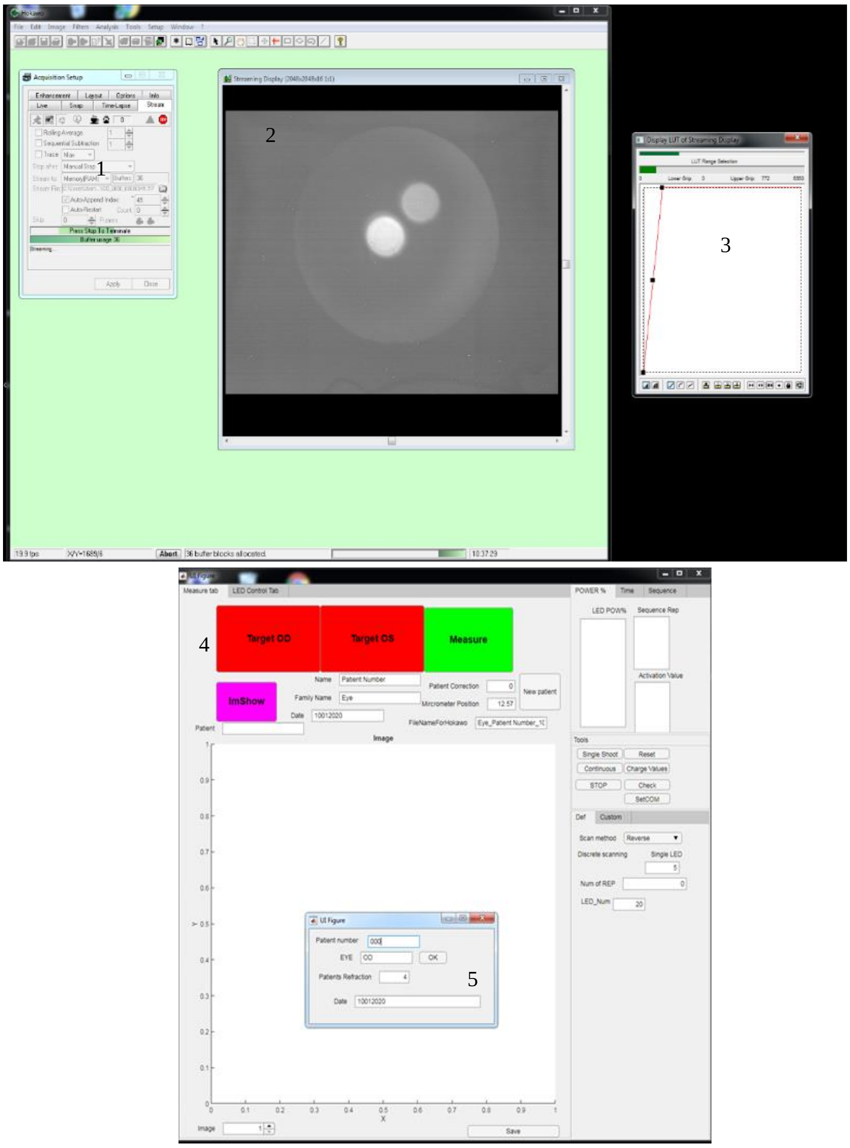

Fig. 2. HoKaWo program ready to take the capture (top). 1: Camera control. 2: visualization during the capture. 3: Window to adjust the Look Up Table (LUT) (right). MATLAB program (bottom). 4: Options to choose the right or left eye and take the photo (“Target UD” / “Target UE” / “Measure”). 5: Window to introduce patient’s information.

2.3 Clinical measurements and protocol

A clinical study was conducted at the University Vision Center (CUV) in Terrassa (Spain) during the months of September, October and November 2019. All patients provided written informed consent before any examination and ethical committee approval was obtained. The study complied with the tenets of the 1975 Declaration of Helsinki (Tokyo revision, 2004).

All patients were examined with the usual tests of optometric consultation, evaluating the best-corrected visual acuity (BCVA), refractive error, intraocular pressure (IOP) with an air-puff tonometer (CT-80, Topcon, Japan) and performing conventional retinography and OCT (3D OCT-1 Maestro, Topcon, Japan).

The inclusion criteria of the study were:

- Age between 30-89 years old.
- Healthy eyes (with an IOP below 21mmHg).

- Subjective refraction between ±15D and astigmatism ≤2D (spherical refraction limited by the prototype correction range and low astigmatism value to obtain acceptable images without high distortion).

Before the acquisition of the images of the fundus, the alignment and LUTs were set by means of the two programs and the micrometric screw described in the former section, and an additional background image was also taken to remove some artefacts coming from the system (internal reflections, stray light, etc.) using a black blanket placed in front of it to avoid any ambient light entering inside (Fig. 3).

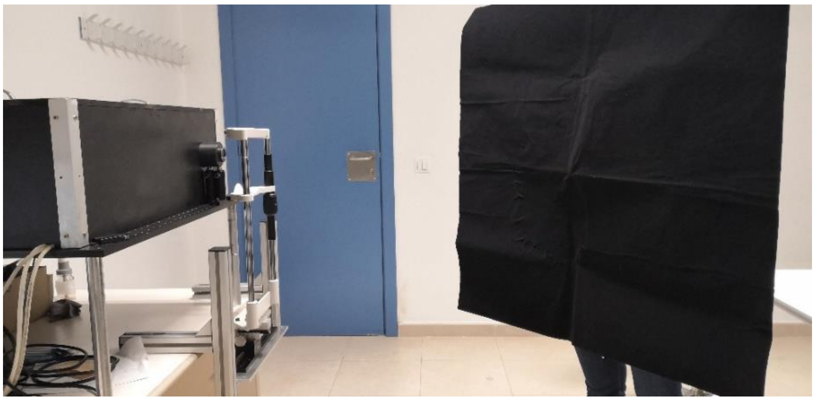

Fig. 3. Acquisition of the background image with the black blanket with the room in the dark.

Then, in order to capture the fundus images, the patient was asked to place the chin and front at the chinrest, looking at a red square fixating point (available inside the prototype, one for each eye). Through the manual adjustment of the chinrest, the acquisition of the images was carried out. The patient was asked not to blink for a few seconds to obtain the whole sequence of spectral images (613ms). In total, two images were taken for each eye and the entire process was done with the light of the room turned off.

3. Results

A total of 120 eyes of 60 patients were measured. Eight of them were excluded from the analysis as they did not comply the age and refraction inclusion criteria; additionally, four more eyes of two patients were excluded for having cataracts and 3 more ones due to the existence of other pathologies. The rest (105) were healthy eyes. However, six of them had been previously implanted with Intraocular Lenses (IOL) during cataract surgery (these were included in the study). Table 1 shows the number of healthy eyes for different groups of age measured (divided in decades of age between 30 and 89 years), and the corresponding mean age, distribution of gender, BCVA and manifest subjective refraction.

Table. 1. Number of healthy patients / eyes for every age group, mean age (years), F: female, M: male, BCVA: best-corrected visual acuity (decimal), Sphere and cylinder (Diopters) included in the study (also those implanted with IOLs).

Age (years)	Mean age	Number of eyes	Gender (%)	BCVA	Sphere	Cylinder
30-39	34 ± 1,633	7	75% F / 25% M	1,057 ± 0,098	-0,321 ± 1,830	-0,571 ± 0,773
40-49	47,192 ± 1,721	26	43% F / 57% M	1,146 ± 0,179	-0,26 ± 1,866	-0,529 ± 0,653
50-59	54,591 ± 2,471	44	59% F / 41% M	0,993 ± 0,219	+0,915 ± 2,582	-0,56 ± 0,453
60-69	65,263 ± 3,246	19	55% F / 45% M	1,011 ± 0,099	+1,789 ± 0,951	-0,434 ± 0,432
70-79	73,5 ± 3,16	5	67% F / 33% M	1,000 ± 0,000	+1,300 ± 1,052	-0,550 ± 0,716
80-89	80 ± 0,00	4	100% F / 0% M	0,975 ± 0,05	+1,125 ± 1,601	-0,625 ± 0,722

Figures 4, 5, 6 and 7 show the fundus images measured for four healthy patients aged 32, 46, 63 and 80 years old, respectively.

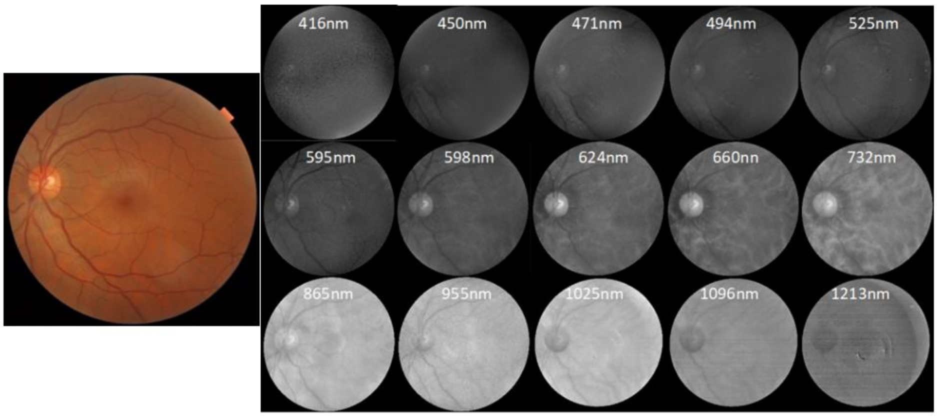

Fig. 4. Images of the patient 087 aged 34 years old. Left: fundus image taken with the OCT Maestro 3D. Right: spectral fundus images obtained with the HYS prototype.

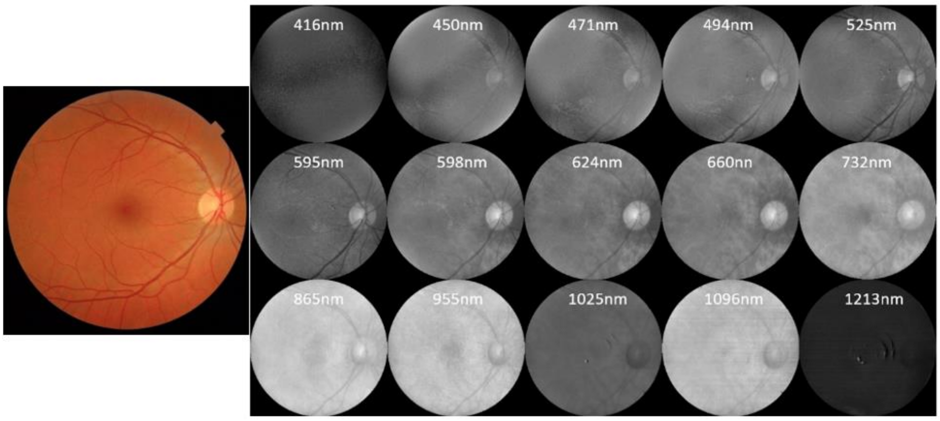

Fig. 5. Images of the patient 025 aged 46 years old. Left: fundus image taken with the OCT Maestro 3D. Right: spectral fundus images obtained with the HYS prototype.

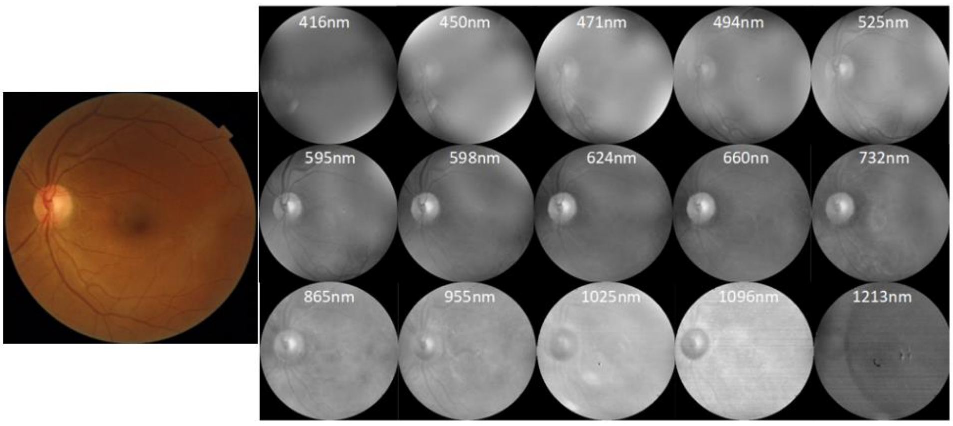

Fig. 6. Images of the patient 002 aged 64 years old. Left: fundus image taken with the OCT Maestro 3D. Right: spectral fundus images obtained with the HYS prototype.

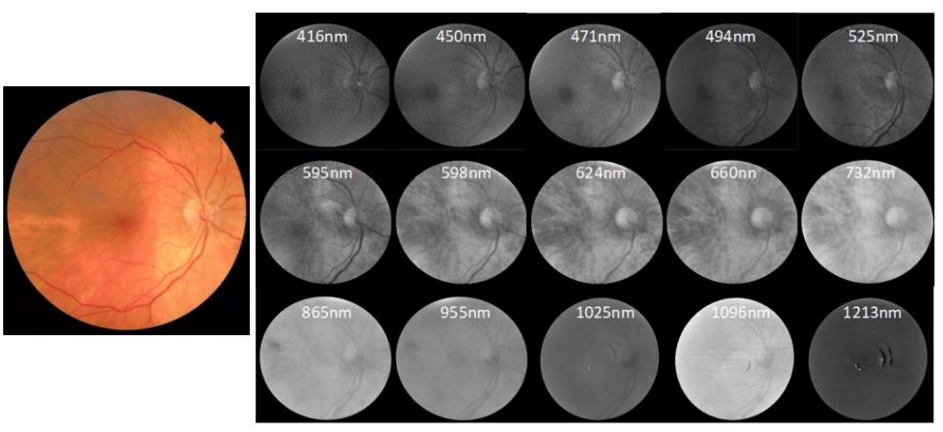

Fig. 7. Images of the patient 090 aged 80 years old. Left: fundus image taken with the OCT Maestro 3D. Right: spectral fundus images obtained with the HYS prototype.

Some details can be further analysed from these examples. For instance, comparing the macular zone of the spectral fundus in the two patients aged 46 and 80 years old, respectively, it can be seen that the fovea of the youngest patient is more defined than that of the older one with has less defined macular limits, especially at medium wavelengths (Fig. 8).

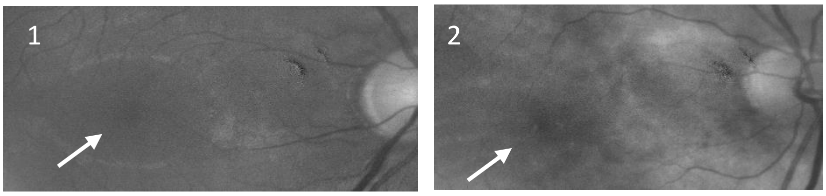

Fig. 8. HYS image taken at 595nm showing the macular area. 1: patient aged 46 years old. 2: patient aged 80 years old.

In reference of the ONH and the excavation, we can see that with age, the edges are less defined. Figure 9 shows zoomed images taken at 660nm of the ONH of the four healthy patients aged 34, 46, 64 and 80 years old, respectively. As it can be seen, in the image of the oldest patient (4) the ONH edges are blurred and the excavation cannot be easily observed, while in the other patients the edge's delimitation is well defined.

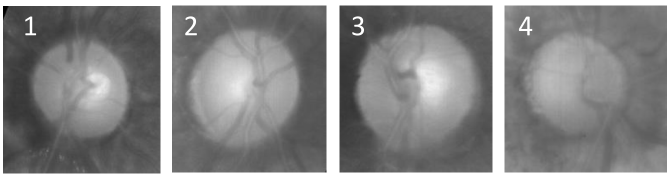

Fig. 9. HYS image taken at 660nm. 1: patient aged 34 years old. 2: patient aged 46 years old. 3: patient aged 64 years old. 4: patient aged 80 years old.

In regards with the observation of nervous fibers, figure 10 shows spectral images taken at 471nm, where the comparison of these more superficial zones can be better carried out. It can be seen that in the image corresponding to the youngest patient (1), the nervous fibres are clearly visible, whereas in the oldest one (4) they are not so evident.

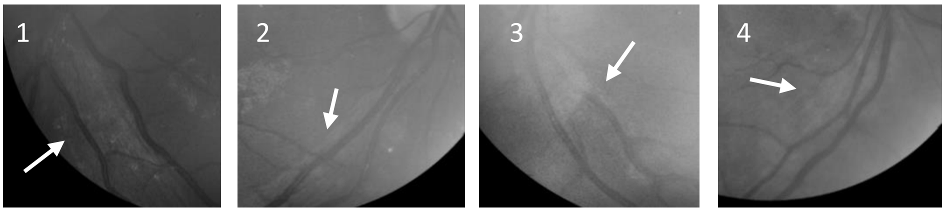

Fig. 10. HYS image taken at 471nm. 1: patient aged 34 years old. 2: patient aged 46 years old. 3: patient aged 64 years old. 4: patient aged 80 years old.

In the following paragraphs, an analysis of the observed retinal structures in spectral images as a function of the wavelength (like nervous fibres, blood vessels and choroidal vasculature) is done. Figure 11 shows zoomed colour and spectral images taken at 471nm, 494 nm and 525 nm of the patient 087 aged 34 years. In the monochromatic spectral images, the nervous fibres can be more clearly distinguished than using the coloured one, as at these short wavelengths light is reflected more superficially in the eye fundus than at longer ones.

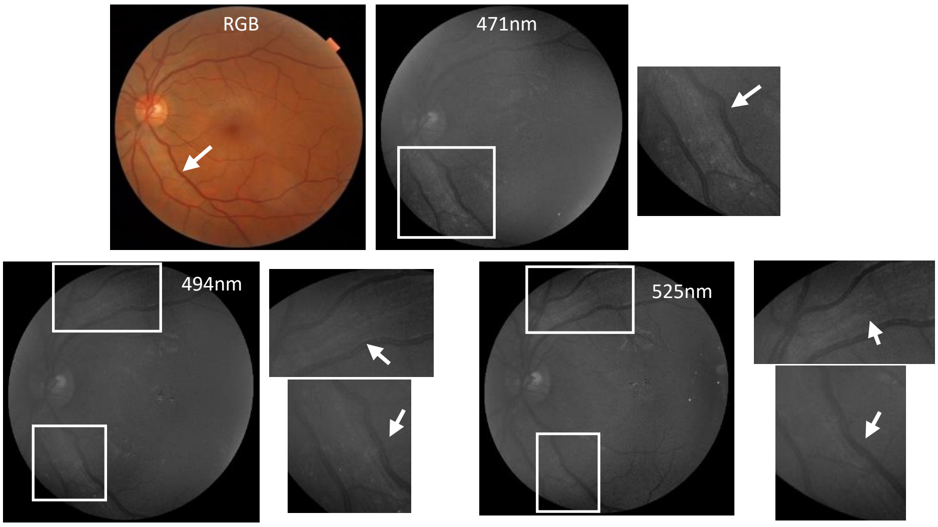

Fig. 11. Images of the patient 087 aged 34 years old. Left: fundus image taken with the OCT Maestro 3D. Spectral fundus images obtained with the HYS prototype at 471nm, 494nm and 525nm. White arrows: nervous fibers.

Figure 12 shows spectral images taken at 471 nm, 595 nm and 865 nm for patient 090 aged 80 years. In the monochromatic spectral images corresponding to intermediate wavelengths, the retinal blood vessels can be more clearly distinguished than using the others as haemoglobin absorbs stronger at blue and green peaks.

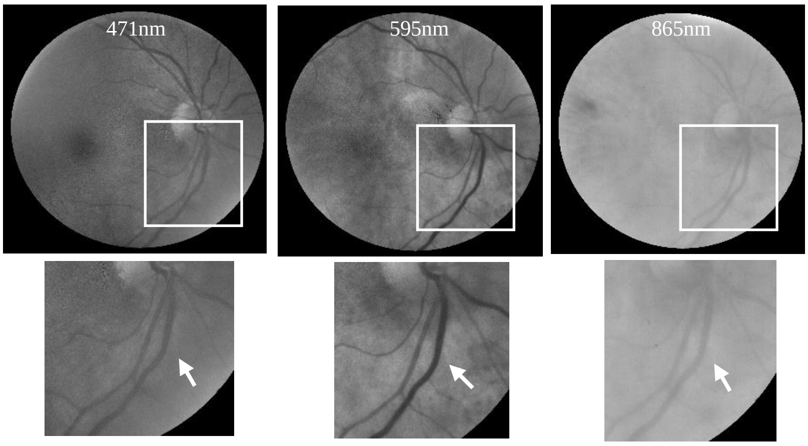

Fig. 12. Images of the patient 090 aged 80. Fundus image taken with the OCT Maestro 3D (RGB). Spectral fundus images obtained with the HYS prototype at 471nm, 595nm and 865nm.

On the other hand, figure 13 shows the HYS images taken at 732nm and 955nm for patients 087 and 025 aged 34 and 46 respectively. As expected, light penetrates deeper at longer wavelengths and therefore, information from deeper layers as the choroid and its vasculature is available at images within the NIR extended spectral range of the HYS prototype used.

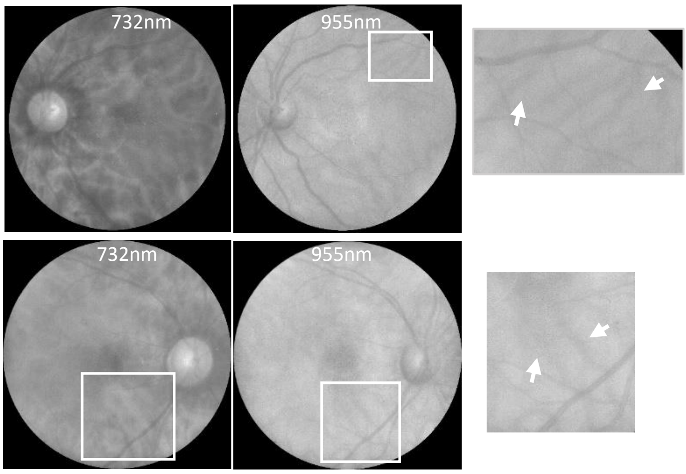

Fig. 13. Images of the patient 087 (top) and 025 (bottom) aged 34 and 46, respectively. Spectral fundus images obtained with the HYS prototype at 732nm, and 955nm. White arrows: choroidal vasculature.

Besides the healthy eyes analysed so far, the following figures show examples of pathologic eyes that were excluded from this study. Figure 14 corresponds to a patient of 67 years old with cataracts. As it can be seen, in the images taken at short wavelengths (416nm – 494nm), retinal structures, such as the blood vessels, choroidal vasculature, among others, cannot be distinguished.

On the other hand, figure 15 shows the left eye of a patient aged 78 years old, who was diagnosed with myopic choroiditis. This ocular disease is based on a set of signs associated with myopia. The principal damage is the presence of chorioretinal atrophic areas. As it can be seen at the zoomed colour and OCT records, the choroid thickness and colour intensity is irregular and brighter and darker zones can be observed, especially at intermediate (green and red) wavelengths.

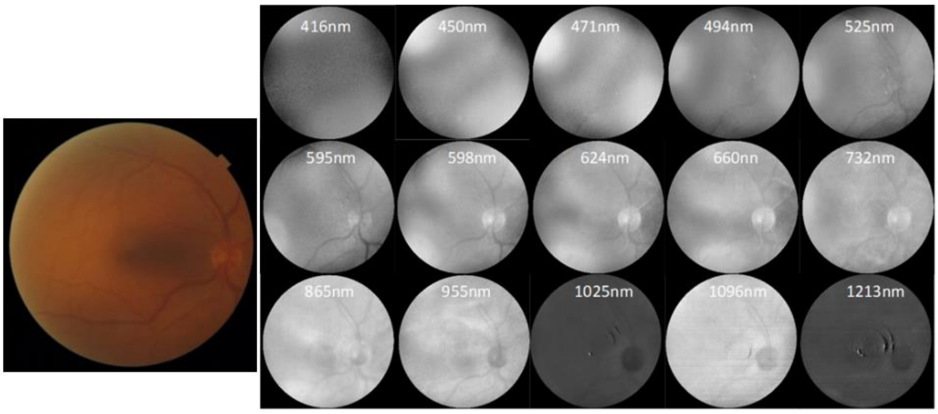

Fig. 14. Images of an eye with cataracts corresponding to the patient 070 aged 67 years old. Left: fundus image taken with the OCT Maestro 3D. Right: spectral fundus images obtained with the HYS prototype.

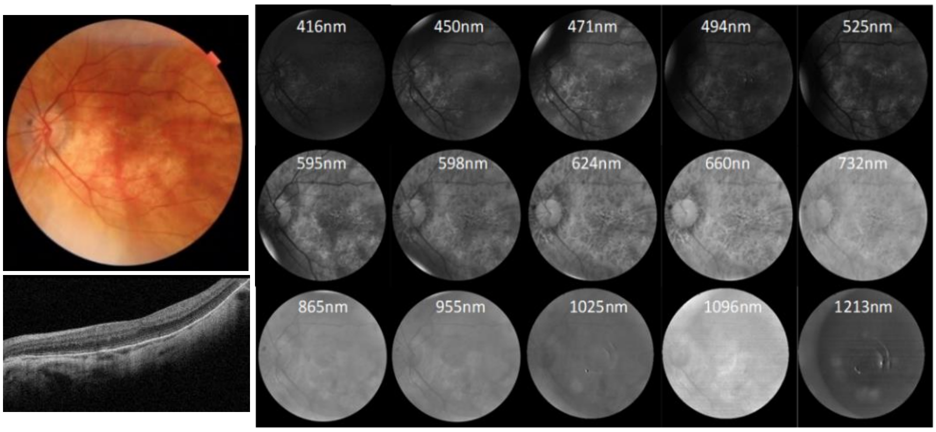

Fig. 15. Images of the patient 022 aged 78 years old diagnosed with myopic choroiditis. Left: fundus image and OCT image taken with the OCT Maestro 3D. Right: spectral fundus images obtained with the HYS prototype.

Finally, in figure 16, the averaged spectral reflectance curves as a function of age (decades of age) corresponding to different retinal structures are shown. These spectral reflectance curves were additionally computed from the digital levels of the images previously shown. Information for the following ocular structures are given: the optic disc, veins, arteries and the retina (without structures).

In the plots, it is noticeable how the 70s and 80s curves have a notably higher reflectance at shorter wavelengths in comparison to other age ranges. This can be explained by the fact that all patients included in these two decades of age (70s and 80s) had been previously implanted with IOLs so that their ocular transmittance, especially at the blue-green wavelengths (>550nm), was enhanced. On the contrary, the reflectance curve corresponding to the range of 60s has lower transmittance due to the possible loss of ocular media transparency that takes place with aging. Also, a minimum of reflectance can be observed at the near-infrared (around 1000nm). This is due to the water absorption that mainly takes place in the ocular media in front of the retina (cornea, lens, vitreous and aqueous humour). As it can be seen in figure 17 this has also been observed by other authors [16].

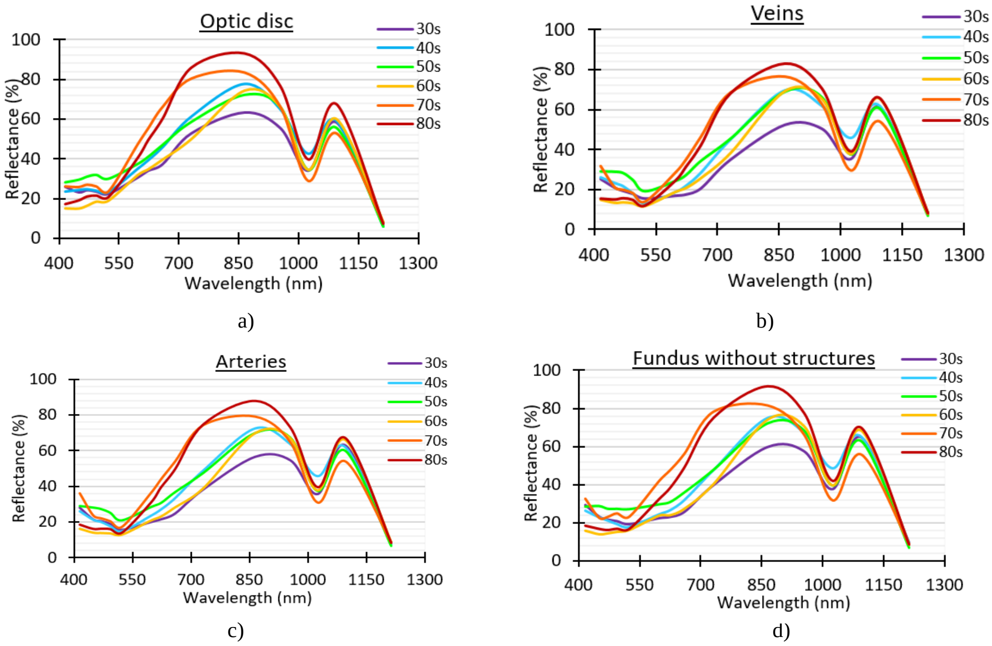

Fig. 16. Absolute spectral reflectance curves of the optic disk (a), veins (b), arteries (c) and fundus without structures (d) as a function of age.

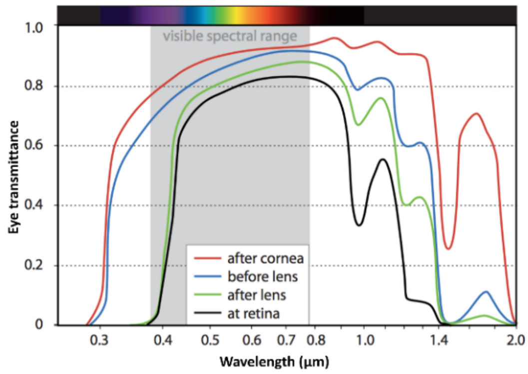

Fig. 17. Spectral transmittance of the eye at different axial locations (Source: Ref. 16).

Figure 18 shows the absolute spectral reflectance curves for the eyes of the patient with myopic choroiditis, which were actually both previously implanted with IOLs. In the plots, and in both eyes, differences of spectral reflectance between dark and bright zones are highlighted. The brighter areas correspond to chorioretinal atrophic areas (lesions) where the reflectance is higher.

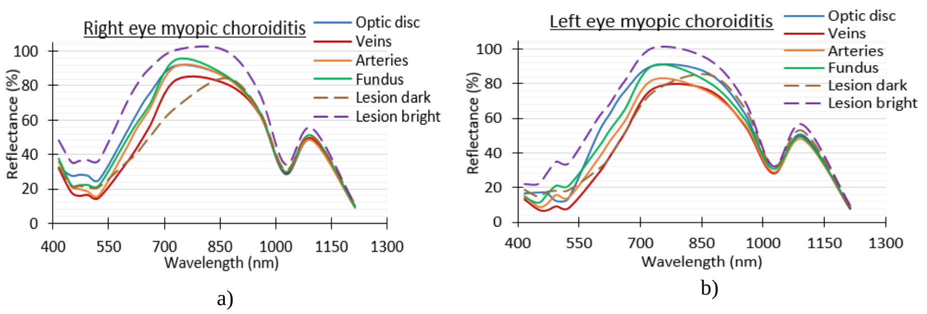

Fig. 18. Absolute spectral reflectance curves of the right (a) and left (b) eyes of patient 022 aged 78 years old diagnosed with myopic choroiditis.

Finally, figure 19 shows the mean absolute spectral reflectance curve corresponding to patients with cataracts.

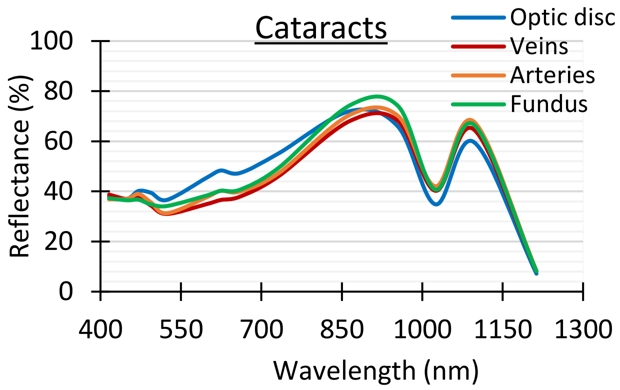

Fig. 19. Absolut spectral reflectance curves of patients with cataracts.

In the plot, it is noticeable the reduction of reflectance, especially in wavelengths up to 850nm. This reduction is caused because of the loss of transparency in the lens (the intraocular diffusion is higher) and also the yellowish effect (the lens acts as a yellow filter absorbing more at the blue wavelengths) that typically appears with a cataract.

4. Conclusions

In this study, we have validated a HYS fundus camera with 15 spectral bands as a means of obtaining spectral information of healthy patients aged from 30 to 80 years old. We obtained spectral images in the VIS and NIR ranges as well as reflectance curves for several ocular structures and for each decade of age considered. Results highlighted the usefulness of the system: for example, patients with IOL implants had higher reflectance at shorter wavelengths, as expected and, therefore, the fundus could be better observed in such patients. The results also showed that, on average, as the age increases, the reflectance between 550nm and 850nm decreases. The HYS images showed some additional information of the fundus in comparison with the obtained using the conventional fundus camera, especially details of the choroid as the NIR wavelengths penetrate deeper due to lower absorption of the tissue. Also, the HYS fundus camera was used to image the fundus of some patients with pathologies, like patients with cataracts or other retinal diseases.

In conclusion, images taken with the HYS system provide additional information that might be clinically relevant to early diagnose some ocular diseases, in which some small signs can be ignored using conventional retinography.

Funding

Spanish Ministry of Economy and Competitiveness (DPI2017-89414-R) and the European Union (BE-OPTICAL: Advanced Biomedical Optical Imaging and Data Analysis (675512).

Disclosures

The authors declare that there are no conflicts of interest related with this article.

Acknowledgements

I am grateful to the University Vision Centre (CUV) and all patients that participated voluntarily in the study. I also thank colleagues Tommaso Alterini, developer of the system, and Estel·la Blanch, who also participated in the study by carrying out clinical measures.

References

[1] H. Hashemi, M. Khabazkhoob, et al., "The Prevalence of Age-Related Eye Disease in an Elderly Population". Rev. Ophthalmic Epidemiology, 24(4), 222–228 (2017).
[2] B. Khoobehi, JM. Beach, et al., "Hyperspectral Imaging for Measurement of Oxygen Saturation in the Optic Nerve Head." Rev. Investigative Ophthalmology & Visual Science, 45(5), 1464–1472 (2004).
[3] M. Yaslam, F. Al Adel, et al., "Non-mydriatic fundus camera screening with diagnosis by telemedicine for diabetic retinopathy patients with type 1 and type 2 diabetes; a hospital-based cross-sectional study" Ann Saudi Med Sep-Oct; 39 (5):328-336 (2019).
[4] A. Ajaz, B. Aliahmad, et al., "Association between Optical Coherence Tomography and Fluorescein Angiography based retinal features in the diagnosis of Macular Edema" Rev. Computers in Biology and Medicine, 116, 103546 (2019).
[5] K. Grieve, E. Gofas-Salas, et al., "In vivo near-infrared autofluorescence imaging of retinal pigment epithelial cells with 757 nm excitation." Rev. Biomedical optics express vol. 9,12 5946-5961. 5 Nov. (2018).
[6] M. Adhi, JS. Duker, et al., "Optical coherence tomography--current and future applications." Rev. Current opinion in ophthalmology vol. 24,3:213-21 (2013).
[7] K. Brown, JM. Sewell, et al., "Comparison of image-assisted versus traditional fundus examination". Rev. Eye and Brain, 1. (2013).
[8] T. Alterini, F. Díaz Douton, et al., "Retinógrafo hiperespectral basado en LEDs para la obtención de imágenes de fondo de ojo en el visible e infrarrojo" Centro de Desarrollo de Sensores, Instrumentación y Sistemas (CD6), Universitat Politècnica de Catalunya (UPC), Terrassa, Barcelona, España (2018).
[9] DJ. Mordant, I. Al-Abboud, et al., "Spectral imaging of the retina," Eye 25(3), 309-320 (2011).
[10] V. Nourrit, J. Denniss, et al., "High-resolution hyperspectral imaging of the retina with a modified fundus camera," J. Fr. Ophtalmol. 33(10), 686-692 (2010).
[11] A. Meshi, T. Lin, et al., "Comparison of retinal pathology visualization in multispectral scanning laser imaging" Rev. Retina, 1, (2018).
[12] NL. Everdell, IB. Styles, et al., "Multispectral imaging of the ocular fundus using light emitting diode illumination," Rev. Sci. Instrum. 81(9), 093706 (2010).
[13] P. Fält, J. Hiltunen, et al., "Spectral imaging of the human retina and computationally determined optimal illuminants for diabetic retinopathy lesion detection," J. Imaging Sci. Technol. 55(3), 030509 (2011).
[14] DJ. Harper, T. Konegger, et al., "Hyperspectral Optical coherence tomography for in vivo visualization of melanin in the retinal pigment epithelium" Rev. Journal of Biophotonics. (2019).
[15] T. Alterini, F. Díaz-Doutón, et al., "Fast visible and extended near-infrared multispectral fundus camera." Rev. J Biomed Opt. Sep;24(9):1-7. (2019).
[16] M. Kaschke, KH. Donnerhacke, et al., Optical Devices in Ophthalmology and Optometry: Technology, Design Principles and Clinical Applications, First. WILEY- VCHVerlag GmbH, (2014).

Universal manuscript template for OSA's journals

AUTHOR ONE,[1] AUTHOR TWO,[2,*] AND AUTHOR THREE[2,3]

[1]*Peer Review, Publications Department, The Optical Society, 2010 Massachusetts Avenue NW, Washington, DC 20036, USA*
[2]*Publications Department, The Optical Society, 2010 Massachusetts Avenue NW, Washington, DC 20036, USA*
[3]*Currently with the Department of Electronic Journals, The Optical Society, 2010 Massachusetts Avenue NW, Washington, DC 20036, USA*
**xyz@osa.org*

Abstract: Word manuscripts submitted to OSA journals as of 30 May 2018 may use these instructions and this new, universal template format. The new template is intended to simplify manuscript preparation and ease transfer between journals. Note that the final published format of OSA journals is not changing at this time. *Applied Optics*, JOSA A, JOSA B, *Optics Letters*, and *Optica* authors may also use the previous, legacy templates, particularly if a precise length estimate is needed. Authors will still need to adhere to article-length restrictions based on the final, published format.

1. Introduction

Adherence to the specifications listed in this style guide is essential for efficient review and publication of submissions. Please note the references should appear at the end of the article after the Funding, Acknowledgements, and Disclosure sections.

2. Page layout and length

Paper size should be U.S. Letter, 21.505 cm x 27.83 cm (8.5 in. x 11 in.). The printing area should be set to 13.28 cm x 21.54 cm (5.25 in. x 8.5 in.); margins should be set for a 3.3-cm (1.3 in.) top/bottom and 4.11-cm (1.625 in.) left/right.

Authors should refer to the Publication Charge page for journal specific information about article processing charges (APCs), open access options, and overlength fees.

3. Typographical style

Please see the checklist in Section 8 that summarizes all of the style specifications.

3.1 Title

Use initial cap for first word in title or for proper nouns. Use lowercase following colon. Title should not begin with an article or contain the words "first," "new" or "novel."

3.2 Author names

Each OSA journal has its own color for the author names. Author names should appear as used for conventional publication, with first and middle names or initials followed by surname. Every effort should be made to keep author names consistent from one paper to the next as they appear within OSA publications.

3.3 Author affiliations

If all authors share one affiliation, superscript numbers are not needed. The corresponding author will have an asterisk correlating to an email address. All authors must have superscripts to callout each affiliation. Hard returns (Enter key) must be used to separate each individual affiliation. Abbreviations should not be used. Please include the country at the end of the affiliation.

AUTHOR ONE[1] AND AUTHOR TWO[2,*]

[1]Peer Review, Publications Department, Optical Society of America, Washington, DC 20036, USA
[2]Publications Department, Optical Society of America, Washington, DC 20036, USA
**opex@osa.org*

Option 1 for affiliation line with two email addresses (only one for the corresponding author):

AUTHOR ONE[1,3] AND AUTHOR TWO[2,*]

[1]Peer Review, Publications Department, Optical Society of America, Washington, DC 20036, USA
[2]Publications Department, Optical Society of America, Washington, DC 20036, USA
[3]xyz@osa.org
**opex@osa.org*

Option 2 for affiliation line with two email addresses (no asterisk used to denote corresponding authorship, implying that the two email addresses share corresponding authorship equally):

AUTHOR ONE[1,3] AND AUTHOR TWO[2,4]

[1]Peer Review, Publications Department, Optical Society of America, Washington, DC 20036, USA
[2]Publications Department, Optical Society of America, Washington, DC 20036, USA
[3]xyz@osa.org
[4]opex@osa.org

3.4 Abstract

The abstract should be limited to approximately 100 words. If the work of another author is cited in the abstract, that citation should be written out without a number, (e.g., journal, volume, first page, and year in square brackets [Opt. Express **22**, 1234 (2014)]), and a separate citation should be included in the body of the text. The first reference cited in the main text must be [1]. Do not include numbers, bullets, or lists inside the abstract.

3.5 Copyright

The line immediately following the abstract should include the copyright statement:

Open access papers should use the following copyright statement:

Authors for *Photonics Research* should use the following copyright statement:

Please be sure to update this line with the appropriate publication year if needed.

3.6 Main text

Section headings may be numbered consecutively and consistently throughout the paper in Arabic numbers and typed in bold. Use an initial capital letter followed by lowercase, except for proper names, abbreviations, etc. Do not include references to the literature, illustrations, or tables in headings.

Subsection headings may be numbered consecutively in Arabic numbers to the right of the decimal point, with the section number to the left of the decimal point as shown in this paper.

Numbering of section headings and subsection headings is optional but must be used consistently throughout papers in which it is applied. *Optics Letters* papers should not have section headers.

3.7 Equations

OSA journals do not accept equations built using the Word 2007 or 2010 Equation Builder. All display equations should be created in MathType (Microsoft Equation Editor 3.0 users are encouraged to use MathType now that Microsoft no longer supports the Equation Editor). Inline equations can be created with these tools or by using keyboard and Unicode characters where needed for the best quality line spacing. We strongly encourage authors to use MathType 6.9. Note that LaTeX users can type LaTeX code directly into MathType for rendering in Word.

Please refer to the online style guide for detailed instructions for including equations in your paper.

4. Figures, supplementary materials, and tables

4.1 Figures

Figures should be included directly in the document. All illustrations must be numbered consecutively (i.e., not by section) with Arabic numbers. The size of a figure should be commensurate with the amount and value of the information conveyed by the figure.

Authors must use one image file per figure. Figures must be inserted as objects that are fixed and move with the text, not as floating objects. Figures should never be placed in a table environment, embedded inside the text, or included within a list. All the figures should be centered. No part of a figure should go beyond the typing area. Place figures as closely as possible to where they are mentioned in the text. Figures should be numbered consecutively in the order of appearance and citation in the text. Be sure to cite every figure.

The abbreviation "Fig." for figure should appear first followed by the figure number and a period.

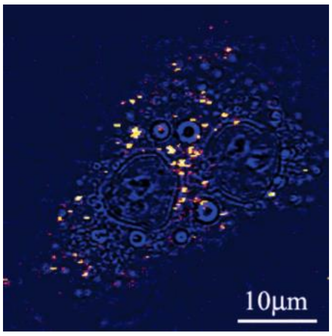

Fig. 1. Sample caption (Ref. [4], Fig. 2).

4.2 Supplementary materials

Supplementary materials uploaded through Prism will be hosted in the OSA figshare portal. The material in figshare will not be publically accessible during peer review. Datasets and code may be uploaded to the OSA figshare portal or be placed in an appropriate external repository. See guidelines below.

Table 1. Supplementary Materials Supported in OSA Journals[a]

Visualization	2D image, 3D image, video
Data File	Small data file such as data underlying a plot in a figure
Dataset	Dataset stored in an appropriate external repository
Code	Code or simulation files stored in an appropriate external repository

[a]*Optica* allows authors to include a supplemental document that can contain additional text, equations, citations, etc. (see Supplementary Materials in *Optica* for details). For all other OSA journals, supplemental text must be included as appendices within the primary manuscript.

Please refer to the Author Guidelines for Supplementary Materials for more detailed instructions and other acceptable supplementary material types.

4.3 Tables

Tables should be centered and numbered consecutively. Authors must use Word's Table editor to insert tables. Authors must not import tables from Excel. All content for each table should be in a single Word table (do not split content for a single table across multiple Word tables). Tables should use horizontal lines to delimit the top and bottom of the table and column headings. Detailed explanations or table footnotes should be typed directly beneath the table, but not in a table cell. Table footnote labels should be alphabetical; numbers or special characters are not permitted. Position tables as closely as possible to where they are mentioned in the main text.

Table 2. Optical Constants of Thin Films of Materials[a]

	83.4 nm		121.6 nm	
Material	n	K	n	k
Ir	1.182	0.865	1.450	1.040
MgF2	1.584	0.487	1.682	0.0627
Al	0.09874	0.1915	0.0424	1.137
Mo	0.98	1.08	0.78	1.03
C	1.16	1.29	1.85	1.10

[a]From Appl. Opt. **40**, 1128 (2001).

5. Funding, acknowledgments, and disclosures

5.1 Funding

Funding information should be listed in a separate block preceding any acknowledgments. The section title should not follow the numbering scheme of the body of the paper. List just the funding agencies and any associated grants or project numbers, as shown in the example below:

National Science Foundation (NSF) (1253236, 0868895, 1222301); Program 973 (2014AA014402); Natural National Science Foundation of China (NSFC) (123456).

OSA participates in Crossref's Funding Data, a service that provides a standard way to report funding sources for published scholarly research. To ensure consistency, please enter any funding agencies and contract numbers from the Funding section in Prism during submission. Update any changes to your funding information in Prism during any revision stages.

5.2 Acknowledgments

Acknowledgments should be included at the end of the document. The section title should not follow the numbering scheme of the body of the paper. Please do not include any funding sources in the Acknowledgment section.

5.3 Disclosures

Disclosures should be listed in a separate section at the end of the manuscript. The section title should read "**Disclosures**" in 10-pt. bold Arial font. The section title should not follow the numbering scheme of the body of the paper. List the Disclosures codes identified on OSA's Conflict of Interest policy page, as shown in the examples below:

ABC: 123 Corporation (I,E,P), DEF: 456 Corporation (R,S). GHI: 789 Corporation (C).

If there are no disclosures, then list “The authors declare no conflicts of interest.”

6. References

References should appear at the end of the article after the Funding, Acknowledgements, and Disclosure sections.

OSA journals use numerical notation in brackets for bibliographic citations. At the point of citation within the main text, designate the reference by typing the number in after the last corresponding word [1]. Reference numbers should precede a comma or period [2]. Two references [3,4], should be included together, separated by a comma, while three or more consecutive references should be indicated by the bounding numbers and an en dash [1–4].

Please refer to the online style guide for detailed instructions on how to format citations for OSA journals.

7. Article thumbnail upload

OSA authors are strongly encouraged to upload a thumbnail image to be used next to their article in the Table of Contents and abstract pages of the journal. Authors must submit a .JPG file. The image will be resized to **100** x **100** pixels. For best results, authors should upload an image this size or an image with **square dimensions**. *No author photos are to be submitted; exceptions must be cleared by the Managing Editor.*

The 100 x 100 pixel image will be displayed on the article abstract page, and a 50 x 50 pixel image will be displayed on the Table of Contents page.

Although a replica of the image does not need to appear in the manuscript itself, it must have a strong connection to the research contained within the paper and must be the property of the author(s) of the current paper. This means that even if the article does not contain figures, a thumbnail can still be submitted as long as it relates strongly to the research and is original. Images containing institution or corporate logos should not be submitted.

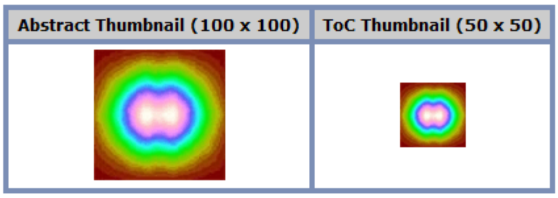

Fig. 2. Preview of thumbnail image display on the author submission page.

8. Summary

Conforming to the specifications listed above is of critical importance to the speedy publication of a manuscript. Authors should use the following style guide checklist before submitting an article.

Table 3. Style Guide Checklist

Standard Page Text Area: 5.25 x 8.5 in.; Margins: 1.3 in. top and bottom, 1.625 in. left and right				
Type of Text	**Font**	**Font Size (Points)**	**Alignment**	**Notes**
Title	Arial	16	Left	**Bold** Spacing expanded by 0.5 pts. Kerning 16 pts
Author Name	Arial	12	Left	**Bold** Use SMALL CAPS Use journal color

Affiliation & Email	Times New Roman	9	Left	*Italic*
Abstract	Times New Roman	10	Justified	Bold "**Abstract:**" header
Copyright	Times New Roman	8	Left	
Main Text First paragraph Subsequent paragraphs	Times New Roman	10	Justified	The first paragraph of a section or subsection is not indented. The first line of subsequent paragraphs is indented 0.2 in.
Section & Subsection Headings	Arial	10	Left	Insert 6-pt. space above and below each heading. Section headers: **Bold** Subsection headers: *Italic*
Equations		10	Center	Eq. Number: right tab to end of last line of Eq., in parentheses.
Figures			Center	
Figure Captions	Times New Roman	8	Justified	Long captions: indent 0.5 in. left/right.
Tables	Times New Roman	8	Center	**Table 1. Bold table captions**
Table Heads	Times New Roman	8	Center	Long heads follow table margins.
Funding	Times New Roman	10	Justified	Bold "**Funding**" section header
Acknowledgments	Times New Roman	10	Justified	Bold "**Acknowledgments**" section header
Disclosures	Times New Roman	10	Justified	Bold "**Disclosures**" section header
References	Times New Roman	8	Left	Bold "**References**" section header

References

1. P. J. Harshman, T. K. Gustafson, and P. Kelley, "Title of paper," J. Chem. Phys. **3**, (to be published).
2. K. Gallo and G. Assanto, "All-optical diode based on second-harmonic generation in an asymmetric waveguide," J. Opt. Soc. Am. B **16**(2), 267–269 (1999).
3. B. R. Masters, "Three-dimensional microscopic tomographic imagings of the cataract in a human lens in vivo," Opt. Express **3**(9), 332–338 (1998).
4. D. Yelin, D. Oron, S. Thiberge, E. Moses, and Y. Silberberg, "Multiphoton plasmon-resonance microscopy," Opt. Express **11**(12), 1385–1391 (2003).
5. B. N. Behnken, G. Karunasiri, D. R. Chamberlin, P. R Robrish, and J. Faist,"Real-time imaging using a 2.8~THz quantum cascade laser and uncooled infrared microbolometer camera,'" Opt. Lett. **33**(5), 440–442 (2008).